Final version at http://ecst.ecsdl.org/content/72/1/105.abstract

Assessing the Advantages of Using Square Wave Signals for Particle Trapping in Carbon-Electrode Dielectrophoresis

Guillermo Contreras-Dávila[a,b], Jose I. Gomez-Quiñones[b], Victor H. Pérez-González[b] and Rodrigo Martinez-Duarte[a]

[a] Department of Mechanical Engineering, Clemson University, Clemson, South Carolina 29631, USA

[b] Electrical and Computer Engineering Department, Tecnológico de Monterrey, Monterrey 64849, México

Here we present an improvement on the trapping efficiency of 3D carbon electrode Dielectrophoresis (carbonDEP) by using alternative signal geometries to the more traditional sine used to stimulate the electrodes. In particular, a square waveform is used. Theoretical analysis was based on the Root Mean Square (RMS) values and the Fourier Series Expansion of these signals. Computational modeling was performed to calculate the DEP force generated by the two signal waveforms and allowed for direct comparison. The trapping efficiency between square and sine signals was then determined experimentally. Given the same experiment characteristics, the use of square signals allows for an improvement in the efficiency when trapping polystyrene particles against a flow.

Introduction

Particle separation techniques such as Dielectrophoresis (DEP) have been gaining increasing importance in a variety of applications such as cell separation (1), clinical analysis (2), separation and filtering of contaminated particles (3). Dielectrophoresis refers to particle motion induced by a DEP force resulting from the interaction of that particle with an electric field gradient. Such required field gradient is usually implemented by immersing electrode arrays in a microfluidic device, although other approaches include the distortion of a uniform electric field around insulating structures positioned between the plates (4). DEP has been demonstrated in the separation of a number of particles including cells (5), bacteria (6), viruses (7) and latex particles (8). Increasing the throughput of such devices is an area of active research. Different fabrication methods exist for the fabrication of DEP devices that allow for optimization of the electrode array, in terms of material and dimensions, and the microfluidic reactor (9). Such devices are mostly polarized with a sinusoidal signal and the use of alternative signal geometries has not been explored in depth. For example, comparing the RMS values (V_{RMS}) of the sinusoidal and square signals, the square signal has bigger magnitude for the same voltage. The effect of the harmonics of a square signal, given by the Fourier series expansion, could also contribute to generate a stronger DEP force at specific frequencies. The purpose of this work is to assess the advantages of using a square signal instead of a sinusoidal signal to polarize a DEP device. Our hypothesis is that the use of square signals will improve the efficiency of a DEP device while trapping targeted particles out of a flow. From a practical point of view

and towards implementing DEP devices in the point of care, the use of square signals will also decrease the complexity and cost of the electronic circuitry. Complex components like operational amplifiers, capacitors or inductors are not needed when generating a square signal.

In this work we present modeling results of square signals performed in COMSOL Multiphysics and Matlab software followed by experimental validation. The experiments were performed using a 3D carbon-electrode DEP (carbonDEP) device and 1.1 µm – diameter polystyrene fluorescent particles. For sinusoidal and square signals, different frequencies, voltages and particle concentrations were tested to have a direct comparison of the effect of square signals on trapping efficiency.

Theory

Dielectrophoresis describe the motion of neutral but polarizable particles due a non-uniform electromagnetic field. The dielectrophoretic force depends on several parameters: the dielectric properties of the media and particle, the frequency and magnitude of applied voltage, and the size of the targeted particle. The DEP force on the particle with an applied AC field is:

$$\vec{F}_{DEP} = 2\pi\varepsilon_m a^3 Re\{f_{CM}\}\nabla^2\vec{E}_{RMS} \quad [1]$$

where ε_m is the permittivity of the medium, a is the radius of the particle, E the electric field and f_{CM} the Clausius-Mossotti factor detailed in equation [2]. This factor depends on the difference between the complex permittivity of the medium and the particle at different frequencies and determines the direction of the particle movement.

$$f_{CM} = \frac{\varepsilon^*_p - \varepsilon^*_m}{\varepsilon^*_p + 2\varepsilon^*_m} \quad [2]$$

the complex permittivity of each material depends on its dielectric constant ε and electrical conductivity σ and takes the form $\varepsilon^* = \varepsilon - j\,\sigma/\omega$, where $j=\sqrt{-1}$ (2) (10) (11).

Our particular interest here is the fact that the DEP force can be negative or positive. It will be negative when the medium is more polarizable than the particle, and positive in the opposite case. In the case of negative DEP, the particle moves away from the regions of high electric field. When positive DEP is implemented, the particle will move towards the highest electric field, which is usually some location on the surface of the electrode. Here, we use positive DEP for particle trapping on the surface of 3D glass-like carbon electrodes.

The importance of the electric field gradient on the magnitude of the DEP force suggests the possibility of maximizing the RMS value by choosing an adequate polarizing signal. Table 1 presents the RMS values of different common signals as calculated using equation [3].

$$V_{RMS} = \sqrt{\frac{1}{T_2 - T_1}\int_{T_1}^{T_2}[f(t)]^2} \quad [3]$$

where (T_2-T_1) determines the period of the signal and *f(t)* determines the shape of the signal.

As detailed in Table I, the V_{RMS} of a sinusoidal signal is given by the amplitude of the signal divided by the square root of 2, while the V_{RMS} of the square signal is given by the total amplitude of the signal.

Table I. The RMS value for sine and square waveforms

Waveform	Equation	RMS value
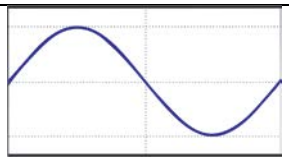 Sine Wave	$f(x) = a\ \sin(2\pi f t)$	$\frac{a}{\sqrt{2}}$
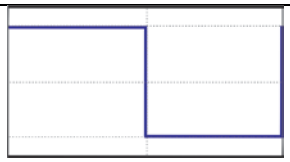 Square Wave	$f(x) = \begin{cases} a & \{ft\} < 0.5 \\ -a & \{ft\} > 0.5 \end{cases}$	a

Furthermore, the harmonics for different signals may contribute to the DEP force. As the Fourier Signal Expansion describe, a periodic function *f(x)* can be represented in term of infinite sum of sines and cosines as shown in equation [4]. Each term in the expansion series is better known as harmonic signal, except the first term called fundamental signal.

$$x(t) = \frac{a_0}{2} + \sum_{n=1}^{\infty} a_n \cos(k\omega_0 t) + b_n \sin(k\omega_0 t) \quad [4]$$

From equation [4], square signals can be represented just as an infinite sum of sine signals because the factors a_0 and b_n becomes zero. The equation to represent a square signal in term of Fourier Series is expressed as:

$$\boldsymbol{x(t) = \frac{4}{\pi} \sum_{n=1}^{\infty} \frac{1}{2n-1} \sin[(2n-1)\omega_0 t]} \quad [5]$$

Where *(2n-1)* factor determine just odd harmonics for square signals. Figure 1 shows the spectral distribution of the fundamental and harmonic signals for this waveform.

As mentioned in the introduction, the effect of the harmonics of a square signal could contribute to generate a stronger DEP force. Based on the mathematical description shown above, each harmonic to a fundamental signal could generate additional DEP forces at its corresponding frequencies. With a single square signal we would expect different DEP forces of decreasing magnitude affecting the same targeted particle at the harmonic frequencies.

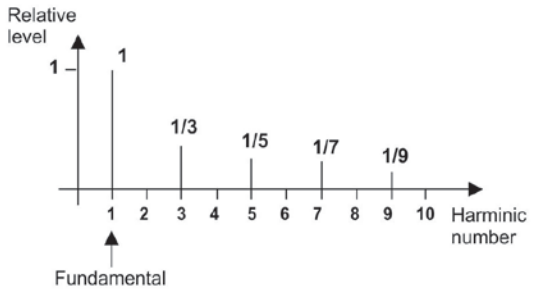

Figure 1. Spectral distribution of a square signal of a specific frequency. The fundamental frequency has an amplitude of 1 while the harmonics at 1/3, 1/5, 1/7, etc. feature a decreasing amplitude.

Materials and methods

Computational modeling

In the computation modeling, COMSOL Multiphysics was used to model the distribution of the electric field gradient generated by RMS value of sine and square signals. Matlab Software was used to calculate the DEP force contribution generated by the harmonics of square signal. In this case, the simulation was performed along a specific frequency range of interest (from 1 kHz to 25 MHz). The frequency range used was selected because within these frequencies we are able to induce positive DEP and negative DEP on 1.1µm polystyrene beads.

The computational modeling was executed in a Windows 7 PC running over an Intel core i3 processor with 4 Gb of memory. The electrodes were assigned a value of 5 V_{pp}. The conductivity of the media (DI Water) was 2.1 µS/m and the particle's conductivity used follows the model shown in the work of O'Konski (12) for solid homogeneous spherical particles where the conductivity of the particle is $\sigma_p = \sigma_b + 2K_s/a$, where σ_b is the bulk conductivity ($\sigma_b \approx 0$), K_s is general surface conductance (typically 1 nS for latex particles) and a the particles radius. The relative permittivity of the media and particles were taken as 80 and 2.3 respectively.

Experimental Materials

Yellow-green fluorescent polystyrene particles with a 1.1µm diameter were purchased from Magsphere Inc® (Part no. PSF-001UM). The experimental sample was a dispersion of these particles in DI water media. The media featured an electrical conductivity of 21 µS/cm. Different particle concentrations were used. The same media without particles was used as detailed in the experimental protocol below.

A carbon-DEP device was used to implement the experiments. The fabrication process of this device has been detailed before (13). Briefly, a SU-8 structure is obtained using photolithography and then carbonized at 900 C in a nitrogen atmosphere. The resultant array of carbon posts and their connecting planar leads are then embedded in a

microfluidics channel. This channel is fabricated using xurography of a double-sided pressure-sensitive adhesive as detailed before by Islam and co-authors (14). The chip used in this work is shown in Figure 2a along with a representative schematic of the electrode array and the area of analysis. Intercalated rows of carbon electrodes are featured. The cross section of the DEP-active area and the materials used is shown in Figure 2b. The carbon electrode array features posts of 50 µm diameter and 100 um height.

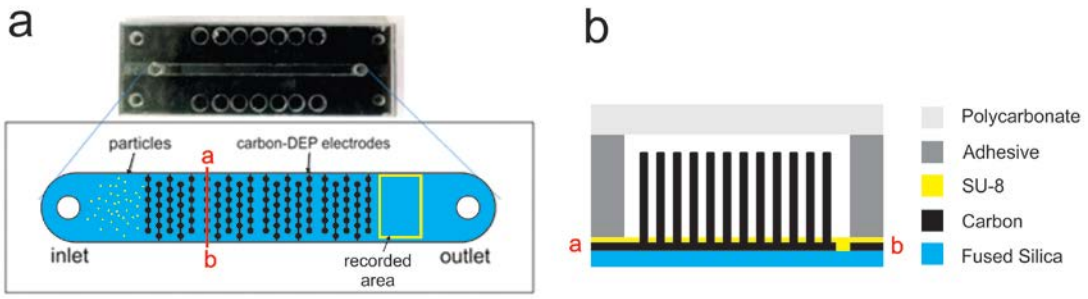

Figure 2. a) Carbon-DEP Chip and schematic used in the experimentation b) Cross section of the Carbon-DEP Chip from a to b and materials composition.

Experimental Protocol

The carbonDEP chip was mounted on a custom-made platform that allowed for connection between a signal generator (BK Precision® 4054) and the chip using push-pins. The fluidic connections were made using polymer tubing and commercial fluidic connectors from IDEX Healthsciences. The experiment was visualized using a CCD camera (Andor® Zyla sCMOS) coupled to a Nikon® Eclipse LV100 upright microscope. The goal of the experiments was to quantify the level of particle trapping in the electrode array under different conditions. Hence, we measured the level of fluorescence in the region immediately after the exit of the electrode array as illustrated in Figure 2a. This region will be referred to as analysis area. The rationale was that the fluorescence intensity would be zero, or the value of a base line, when the array traps all fluorescent particles; and that this level would significantly increase upon the release of the trapped particles after turning the polarizing signal off. The magnitude of this step will then allow for the quantification of the trapping efficiency of the device and enable comparison between the use of sinusoidal and square signals. The experiment started by filling the channel with the particle suspension. At this point, a picture of the analysis area was taken to serve as normalizing point for each experiment. A given flow rate was then established in the device using a syringe pump (Chemix Fusion 100, USA) and the electrode array polarized with a signal of given shape, frequency and magnitude. A sample volume of 100 µl was flowed through the polarized array. After this, 10 µl of media without particles were flowed to wash away un-trapped particles. Following such wash, the polarizing signal was turned off to release all particles. Video, as a stack of images, of the analysis area was recorded for 10 seconds before turning the signal off and 50 seconds afterwards to obtain a 1 minute-long video for each experiment. The focus was to quantify the change of fluorescent intensity in the analysis area just before and after turning the signal off. Experiments for each set of conditions were repeated at least three times.

The parameter of interest in these videos is the fluorescence level in the analysis area which can be measured as the mean gray value. The mean gray value has a scale between 0 and 255, which 0 is total darkness and 255 is total brightness of the image. ImageJ software was used to analyze specific frames of the different videos. These numerical values were then normalized against initial conditions in the channel to obtain the relative fluorescence intensity throughout the experiment. The plots presented below are the result of the direct comparison between the fluorescence intensities right before and after turning the polarizing signal off after the wash.

Results and Discussion

Numerical Modeling

The gradient of the electric field around a simulated carbon electrode is shown in Figure 3. The polarizing voltage is arbitrarily set at 5 V_{pp}. The goal of this simulation was to understand the differences in the field gradient distribution and magnitude when using sinusoidal or square signals. The gradients generated by sinusoidal and square signals are shown in Figure 3a and 3b respectively. The electric field gradient is given in units of $m*kg^2/(s^6*A^2)$ and the magnitude is shown here in a logarithmic scale. It can clearly be discerned than the use of a square signal generates a bigger region of maximum gradient magnitude (in red) around the post. By comparing the volume of maximum gradient between the two cases, an increase of volume of 99% is obtained when choosing square over sinusoidal signals.

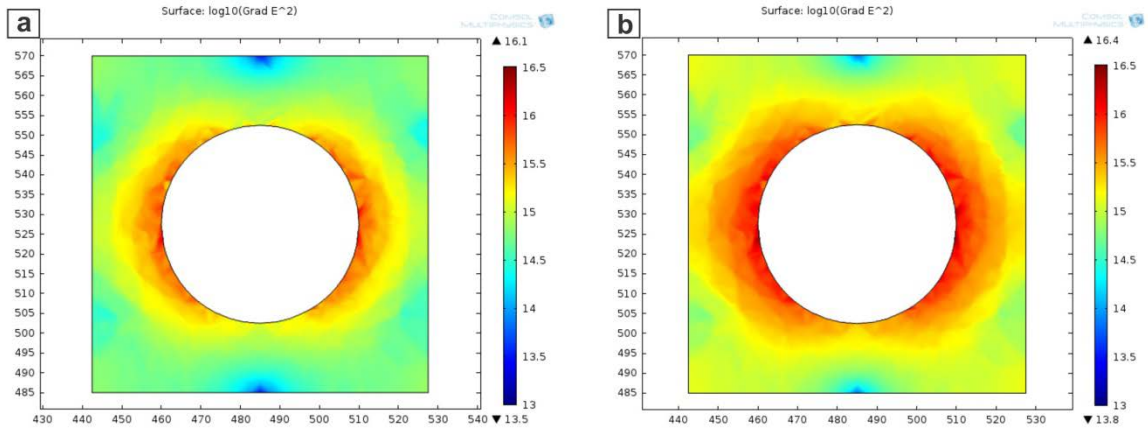

Figure 3. a) Modeling of $gradE^2$ for 5 V_{RMS} sinusoidal signal. b) Modeling of $gradE^2$ for 5 V_{RMS} square signal.

Force modeling using Matlab

The DEP force generated by a single sinusoidal (or fundamental) signal and the DEP force generated by the square signals (or total) at the same voltage amplitude are compared in Figure 4. The red line on the figure shows the gain percent taking on base the DEP force

generated by the sine signal. For frequencies below 28 kHz, the force maintains constant, it does not change with the frequency. The square signal is able to generate around 19% more force than the sinusoidal signal. As the frequency increase, the difference in forces starts decreasing until the frequency in which the DEP force of square signal is equal to the DEP force of sinusoidal signal. This happen approximately at 127 kHz causing a negative gain (red line).

From 127 kHz to 550 kHz, the gain computed was negative. At these frequencies, the DEP force generated by sinusoidal signal is stronger than the generated by the square signal. For frequencies above 550 kHz the DEP forces becomes negative. As the frequencies increase, the DEP force generated by the square signal becomes more negative than the generated by sine signal, reaching a gain of 19% between the two forces. It is important to mention that the cross-over frequency in the Clausius-Mossotti factor is at 550 kHz for the characteristics of the experiment.

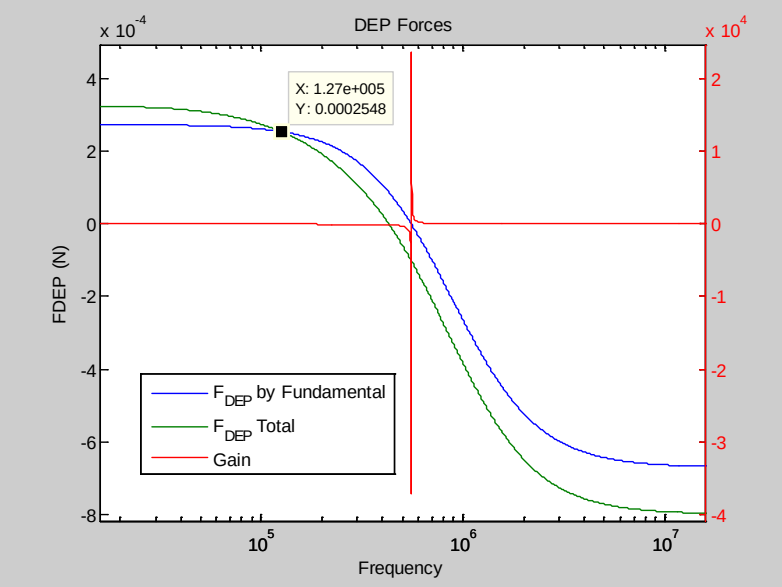

Figure 4. DEP Force and gain for wide frequency range

Frequency change

The first experiments were performed with a fixed particle concentration of 10^8 particles/ml and using a 5 V_{pp} signal amplitude. A frequency sweep was made for each waveform, sinusoidal or square, through the values of 100 Hz, 500 Hz, 1 kHz, 5 kHz, 10 kHz, 100 kHz and 1 MHz. The results comparing particle trapping when using either signal are shown in Figure 5a. Blue and red bars represent the case for sine and square signals respectively. The magnitude of intensity in the Y-axis is the value calculated by subtracting the intensity right before turning the field off from the value right after the polarizing signal is turned off. The taller the bar, the better trapping efficiency.

Only frequencies below 5 kHz lead to positive DEP of the specific latex particles used

here, making it possible to trap particles around the posts. At 5 kHz, particle trapping was only observed in the case of the square signal. A difference between the trapping using sinusoidal and square signal was observed at all frequencies below 5 kHz. The difference is widest when using a frequency of 1 kHz, in which case the trapping when using a sine signal is only 15% of that obtained with a square signal. The difference is the narrowest at 100 Hz. At frequencies lower than 1 kHz, electrothermal flows were observed. This phenomenon disturbs the experiment producing a decrease on the amount of trapping. A vortex-like movement was observed around the posts. The speed of the particle movement in the vortex was observed to be inversely proportional to the signal frequency. As the frequency approximates 10 Hz, the particles can be seen to move back and forth between electrodes following the signal frequency. Although modeling of the DEP force for these latex particles predicted uniform trapping at frequencies below 10 kHz, it is clearly seen from our experimental results that the trapping efficiency decreases according to frequency. We believe the phenomena described for low frequencies are to blame for a decrease in trapping efficiency.

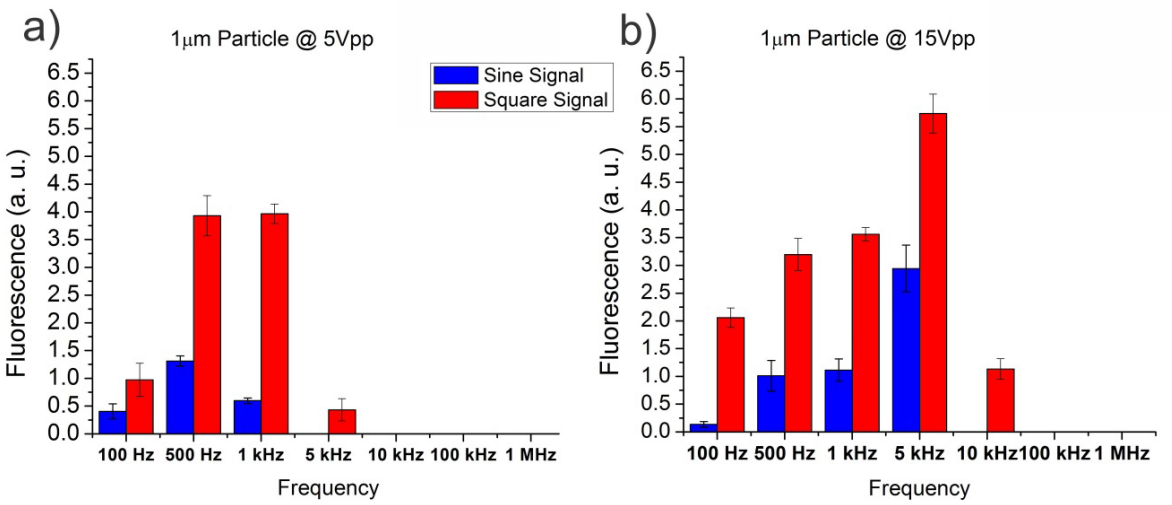

Figure 5. Frequency sweep results at a) 5 V_{pp} b) 15 V_{pp}

Voltage change

In this case the voltage values tested were 1 V_{pp} and 15 V_{pp} in addition to the 5 V_{pp} case shown above. The particle concentration was kept uniform at 10^8 particles/ml, as well as a constant flow rate of 20 µl/min. A similar frequency sweep than that above was implemented. Results are shown in Figure 5b. No discernible trapping was observed at 1 V_{pp}. However, at 15 V_{pp} trapping was possible up to frequencies of 10 kHz, albeit only when using square signals. Frequencies higher than 10 kHz do not lead to particle trapping. The highest different is at 100 Hz where the difference is 9%. This is comparison to 15% obtained at 1 kHz for the 5 V_{pp} case. To have a comparison about how the voltage applied and flow rate modified the volume of trapped particles, an experiment with a small flow rate was performed using both waveforms. The relation Voltage-Flow Rate will show the gain between the two waveforms keeps at fixed frequencies using different voltages or flow rates. The initial flow rate was 20 µl/min at 15 V_{pp}, the proposed experiment was 6.66

µl/min at 5 V_{pp} to have the same ratio: $\frac{15\ V_{pp}}{20\ \mu l/min} = \frac{5\ V_{pp}}{6.66\ \mu l/min}$. The results are shown in Figure 6. The bars on the left show the fluorescence magnitude for the experiment at 5 V_{pp} with a flow rate of 6.6666 µl/min. The proportional gain between the sinusoidal and square signal was 214%. It means the square signal induce a force 2.14 times stronger than that induced by a sine and hence enables the trapping of more particles., The two columns on the right part of Figure 6 show the results obtained by experiment with the signals at 15 V_{pp} with a flow rate of 20 µl/min. The gain between the magnitudes on the square signal and the sinusoidal signal was around 200%. Although the fluorescence magnitude is bigger than the magnitude obtained at 5 V_{pp}, the difference between the sinusoidal and square signal remain almost the same proportion.

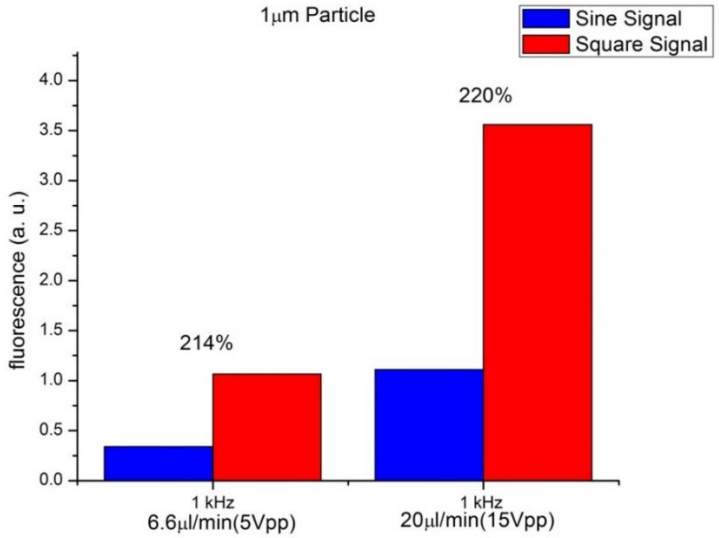

Figure 6. Results for the same relation Voltage-Flow Rate

Conclusion

Here, we demonstrated the advantage of using square signals over traditional sinusoidal signals when trapping fluorescent latex particles. The trapping efficiency using square signals is as much as double as that obtained when using sinusoidal signals. Moreover, a square signal is easier to generate using portable electronics than a sinusoidal signal, and will facilitate future implementation of a hand-held lab-on-a-chip for particle trapping and sorting using carbon-electrode dielectrophoresis. The presented hypothesis about the impact of harmonics on the DEP force requires further experimentation to be able to draw a conclusion. Ongoing work is on implementing extraction of targeted cells from a heterogeneous population using square signals. Future work is on understanding why exactly a square signal leads to improved trapping and exploring other signal geometries.

Acknowledgments

The authors are grateful to the personnel of the Multiscale Manufacturing Laboratory in Clemson University, specially Monsur Islam and Rucha Natu, for their help implementing

the experiments. GC acknowledges support from CONACYT during his visit to Clemson University.

References

1. L. Zheng, J. P. Brody, and P. J. Burke, *Biosens. Bioelectron.*, **20**, 606–619 (2004).
2. P. Tabeling, *Introduction to Microfluidics*, Oxford University Press, Paris, (2005).
3. H. Andersson and A. Van den Berg, *Sensors Actuators, B Chem.*, **92**, 315–325 (2003).
4. S. K. Srivastava, A. Gencoglu, and A. R. Minerick, *Anal. Bioanal. Chem.*, **399**, 301–321 (2011).
5. H. a Pohl and J. S. Crane, *Biophys. J.*, **11**, 711–727 (1971).
6. M. D. C. Jaramillo, E. Torrents, R. Martínez-Duarte, M. J. Madou, and A. Juárez, *Electrophoresis*, **31**, 2921–2928 (2010).
7. M. P. Hughes, H. Morgan, F. J. Rixon, J. P. Burt, and R. Pethig, *Biochim. Biophys. Acta*, **1425**, 119–126 (1998).
8. Z. Dong, *Design*, 1–5.
9. R. Martinez-Duarte, *Electrophoresis*, **33**, 3110–3132 (2012).
10. B. Kirby, *Micro- and Nanoscale Fluid Mechanics: Transport in Microfluidic Devices*, Cambridge University Press, Cambridge, (2010).
11. P. R. C. Gascoyne and Jody Vykoukal, *Electrophoresis*, **23**, 1973–1983 (2002).
12. C. T. O'Konski, *J. Phys. Chemestry*, **64**, 605–619 (1960).
13. R. Martinez-Duarte, P. Renaud, and M. J. Madou, *Electrophoresis*, **32**, 2385–2392 (2011).
14. M. Islam, R. Natu, and R. Martinez-Duarte, *Microfluid. Nanofluidics*, **19**, 973–985 (2015).